

New Highly CO₂-Philic Diglycolic Acid Esters: Synthesis and Solubility in Supercritical Carbon Dioxide[†]

Hai-Jian Yang,^{*,‡} Jia Tian,[‡] and Hakwon Kim^{*,§}

Key Laboratory of Catalysis and Materials Science of the State Ethnic Affairs Commission & Ministry of Education, Hubei Province, Key Laboratory of Analytical Chemistry of the State Ethnic Affairs Commission, College of Chemistry and Materials Science, South-Central University for Nationalities, Wuhan, 430074, P. R. China, and Department of Applied Chemistry and Industrial Liaison Research Institute, College of Applied Science, Kyung Hee University, Gyeonggi 446-701, Republic of Korea

A series of diglycolic acid esters, potent CO₂-philic chelating agents, were designed and synthesized. The solubilities of these compounds in supercritical CO₂ were determined at temperatures from (313 to 333) K and pressures from (8.6 to 20.4) MPa. All of the synthesized esters showed good to high solubility (as high as $1.6 \cdot 10^{-2} \text{ mol} \cdot \text{L}^{-1}$ for compound **1** at 9.3 MPa and 313 K) in supercritical CO₂ at easily accessible temperatures and pressures. To confirm the tested solubility, two density-based correlations proposed by Bartle and Chrastil were investigated for the seven glycolic acid esters. The results showed good self-consistency of the data calculated by the Bartle semiempirical equation and differed from the measured values by between (4 and 37) %. Better agreement with experimental solubility data is obtained with the Chrastil model, and values of AARD lower than 11 % were observed. Solubility data were also used to estimate the partial molar volume \bar{V}_2 for each diglycolic acid ester in the supercritical phase using the theory developed by Kumar and Johnston.

Introduction

Supercritical fluids (SCFs) have an increasing number of applications in dyeing, food, and pharmaceutical industries, separation processes, and catalytic and enzymatic reactions.^{1–3} Supercritical carbon dioxide (scCO₂) is one of the most commonly used supercritical solvents because it is an easy gas to handle, nontoxic, chemically inert, and nonflammable and it has moderate critical constants ($T_c = 31.3 \text{ }^\circ\text{C}$, $P_c = 7.38 \text{ MPa}$), variable density, higher diffusion coefficient, and lower viscosity. Although supercritical fluid solvents possess many desirable features for several fields, the development of new processes has been hindered by lack of engineering data and thermodynamic models. Solubility information of compounds is essential for choosing a supercritical fluid process.^{4,5}

On the other hand, despite its inherent physical property advantages, CO₂ is a nonpolar molecule with a low dielectric constant and low polarizability per unit volume, which limits its ability to dissolve many polar compounds such as water, ureas, amides, ionic species, proteins, sugars, etc.^{6–8} Although CO₂ was not a particularly strong solvent, researchers observed that it could be used to dissolve large quantities of some classes of compounds, including fluorinated materials, silicones, and certain Lewis bases. Therefore, modifying the high molecular weight polar compounds with fluoroether, fluoroalkyl, or silicone groups does greatly increase the solubility in CO₂.^{9–11} Compounds which have a perfluoroalkyl polyether (PFPE) tail show high solubilities in supercritical CO₂ (scCO₂), but this type of compounds is expensive and toxic. Silicone-functional amphiphiles require higher pressure to generate a single-phase solution in scCO₂. It has also been found that the addition of a small amount of alkyl alcohols as single or mixed organic cosolvents to an SCF can dramatically enhance its solvent power, and many papers have been published on this

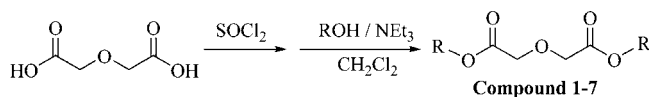
topic.^{3,12} However, in the process of application, this approach must be confronted with the problem of separation once again.

According to the literature,^{13–16} the straight alkyl is a good CO₂-philic group. The alkyl, the carbonyl, and the ether groups were chosen as the CO₂-philic parts which are low cost, nonfluorous, and nonsilicone. In the present work, we have designed and synthesized a series of diglycolic acid esters which would be a potent CO₂-philic chelating agent, and the solubility test work in scCO₂ was carried out over the pressure range from (8.6 to 20.4) MPa and at the temperature of (313, 323, and 333) K, and the tested results were correlated by two density-based correlations (Bartle and Chrastil models). Furthermore, the solubility data were also employed for the estimation of partial molar volumes of the seven diglycolic acid esters in the scCO₂, according to the theory developed by Kumar and Johnston.

Experimental Section

Chemicals and Apparatus. Diglycolic acid ($w = 0.98$, mass fraction), 1-butanol ($w = 0.99$), 1-hexanol ($w = 0.99$), 1-octanol ($w = 0.99$), and 1-decanol ($w = 0.99$) were bought from Alfa Aesar Chem. Co. 1-Dodecanol ($w = 0.99$), 1-tetradecanol ($w = 0.99$), and 1-hexadecanol ($w = 0.99$) were purchased from Tokyo

Scheme 1. Synthesis of Compounds 1 to 7



Compounds	R	Full name
1	-CH ₂ (CH ₂) ₂ CH ₃	dibutyl 2,2'-oxydiacetate
2	-CH ₂ (CH ₂) ₄ CH ₃	dihexyl-2,2'-oxydiacetate
3	-CH ₂ (CH ₂) ₆ CH ₃	dioctyl-2,2'-oxydiacetate
4	-CH ₂ (CH ₂) ₈ CH ₃	didecyl-2,2'-oxydiacetate
5	-CH ₂ (CH ₂) ₁₀ CH ₃	didodecyl-2,2'-oxydiacetate
6	-CH ₂ (CH ₂) ₁₂ CH ₃	ditetradecyl-2,2'-oxydiacetate
7	-CH ₂ (CH ₂) ₁₄ CH ₃	dihexadecyl-2,2'-oxydiacetate

[†] Part of the "Sir John S. Rowlinson Festschrift".

* Corresponding authors. E-mail: yanghaijian@vip.sina.com or hwkim@khu.ac.kr.

[‡] South-Central University for Nationalities.

[§] Kyung Hee University.

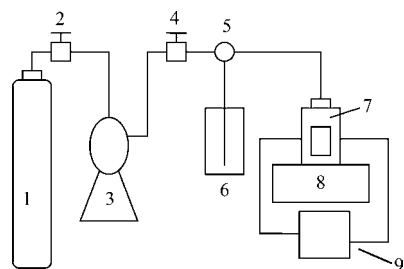


Figure 1. Schematic diagram of experimental apparatus for solubility test in supercritical CO₂. 1, CO₂; 2, 4, two-way valve; 3, “JASCO PU-CO₂” CO₂ delivery pump; 5, three-way valve; 6, “JASCO BP-1580-81” back pressure regulator; 7, view cell with two sapphire windows and a water jacket; 8, magnetic stirrer; 9, water circulator for temperature control.

chemical industry Co. All chemicals were used as received without further purification. Purity CO₂ ($w = 0.9999$, mass fraction) was obtained from Wuhan Steel Co. and used as the fluid.

A “JASCO PU-CO₂” CO₂ delivery pump was used to cool and deliver CO₂ fluid, and a “JASCO BP-1580-81” back pressure regulator was used to keep the pressure in the pressure range of (0 to 35.0) MPa. The temperature was controlled using a temperature controller jacket with an accuracy of ± 0.01 K. IR spectra were measured on a Nexus 470 FT-IR spectrometer. NMR spectra were recorded on a Mercury Plus 400 MHz instrument at ambient temperature using TMS as an internal standard. Elemental analysis was performed by using a PE 2400 series II CHNS/O elemental analyzer.

Table 1. Solubility at Temperature T , Density ρ , and Mole Fraction x for Compounds 1 to 7

T	Compound 1					Compound 2					Compound 3				
	P	ρ	10^4x	10^4x_{cal}	AARD	P	ρ	10^4x	10^4x_{cal}	AARD	P	ρ	10^4x	10^4x_{cal}	AARD
K	MPa	kg·m ⁻³			%	MPa	kg·m ⁻³			%	MPa	kg·m ⁻³			%
313	8.6	380.83	23.34	23.16	0.78	8.4	337.92	19.07	15.74	17.46	8.8	436.05	12.35	10.24	16.71
	8.8	436.05	40.77	40.56	0.52	8.6	380.83	28.21	23.39	17.08	9.0	492.75	18.21	18.07	0.81
	8.9	465.37	57.30	54.66	4.61	8.8	436.05	49.27	39.22	20.39	9.3	556.08	32.28	33.63	4.19
	9.2	538.22	99.09	114.14	15.19	8.9	465.37	69.25	51.66	25.40	9.5	584.52	46.06	44.17	4.12
	9.3	556.08	159.84	136.36	14.69	9.1	517.19	83.08	83.85	0.92	9.6	596.10	60.22	49.26	18.20
323	9.8	363.41	24.46	24.34	0.51	9.5	331.31	19.45	19.60	0.78	10.2	411.27	13.09	13.12	0.24
	10.2	411.27	43.22	38.76	10.32	9.9	374.91	28.65	28.81	0.56	10.5	448.59	20.01	18.75	6.29
	10.5	448.59	59.44	55.85	6.04	10.4	436.22	49.25	49.95	1.41	11.1	515.81	34.80	35.51	2.05
	10.8	484.05	73.45	78.97	7.51	10.7	472.58	68.19	69.27	1.58	11.5	551.56	48.82	49.59	1.58
	10.9	495.10	89.76	87.93	2.04	10.9	495.10	86.79	84.75	2.35	11.9	580.66	61.83	64.73	4.69
333	11.0	359.16	24.75	29.19	17.94	10.6	330.23	19.52	25.49	30.60	11.4	389.65	13.82	17.26	24.90
	11.5	397.42	44.73	41.82	6.50	11.1	366.67	29.30	34.76	18.65	11.8	420.80	21.33	23.00	7.86
	12.0	436.26	61.12	60.41	1.16	11.9	428.55	50.13	59.38	18.44	12.6	480.50	37.36	39.92	6.86
	12.4	466.23	76.26	80.24	5.21	12.1	443.89	58.08	67.84	16.81	13.1	513.54	52.43	54.01	3.02
	12.7	487.42	91.18	97.99	7.47	12.4	466.23	69.12	82.36	19.16	13.7	547.92	65.52	73.67	12.44
T	Compound 4					Compound 5					Compound 6				
	P	ρ	10^4x	10^4x_{cal}	AARD	P	ρ	10^4x	10^4x_{cal}	AARD	P	ρ	10^4x	10^4x_{cal}	AARD
K	MPa	kg·m ⁻³			%	MPa	kg·m ⁻³			%	MPa	kg·m ⁻³			%
313	9.3	556.08	11.40	9.12	20.08	9.2	538.22	6.54	4.65	28.95	10.3	651.49	4.78	4.37	8.95
	9.7	606.40	17.64	15.93	9.72	9.5	584.52	9.56	7.74	19.03	10.7	672.50	7.60	6.48	14.76
	10.2	645.38	24.74	24.12	2.52	9.8	615.65	13.20	10.79	18.20	11.2	693.38	10.57	9.51	10.06
	10.5	662.60	31.60	28.77	8.95	10.0	631.74	16.25	12.77	21.43	11.7	710.44	13.08	12.93	1.16
	10.6	667.69	33.62	30.28	9.91	10.5	662.60	18.73	17.44	6.87	12.5	732.67	14.28	19.11	33.82
323	10.9	495.10	8.50	7.42	12.77	11.2	525.44	6.40	6.47	1.06	13.0	637.96	4.79	5.90	23.20
	11.5	551.56	13.99	13.78	1.46	11.4	543.31	9.17	7.84	14.54	13.6	660.67	7.75	8.99	16.04
	11.8	573.93	18.62	17.54	5.78	11.7	566.85	10.78	10.05	6.76	14.0	673.70	9.99	11.42	14.35
	12.3	604.62	27.57	24.27	11.97	11.9	580.66	13.90	11.62	16.42	14.3	682.60	14.04	13.43	4.34
	13.2	646.02	35.18	37.06	5.34	12.8	629.33	17.32	19.08	10.17	14.6	690.88	15.38	15.60	1.38
333	13.5	537.09	13.23	18.72	41.52	12.8	494.19	6.81	7.42	9.02	15.1	609.28	5.13	6.04	17.70
	13.9	558.17	18.13	23.38	28.96	13.4	531.44	10.14	10.96	8.08	15.7	629.64	9.81	8.82	10.06
	14.2	572.52	23.72	27.16	14.48	14.1	567.87	15.67	15.95	1.76	16.1	641.78	11.68	11.05	5.39
	14.8	597.96	29.20	35.29	20.87	14.2	572.52	16.30	16.72	2.56	16.6	655.62	13.35	14.24	6.72
	15.2	612.88	34.24	41.06	19.93	14.5	585.74	18.20	19.11	4.50	16.9	663.32	14.70	16.39	11.54
T	Compound 7														
	P	ρ	10^4x	10^4x_{cal}	AARD										
K	MPa	kg·m ⁻³			%										
313	13.4	752.90	4.16	4.95	18.77										
	14.5	773.23	6.26	7.06	12.88										
	15.1	782.87	7.95	8.34	4.87										
	16.2	798.61	9.10	10.89	19.58										
	18.1	821.49	11.61	15.90	36.97										
323	15.6	714.89	5.16	6.47	11.34										
	16.0	723.27	7.02	7.84	4.48										
	16.9	740.21	10.95	10.05	16.73										
	17.6	751.91	12.54	11.62	10.34										
	18.4	764.02	14.82	19.08	5.93										
333	17.3	672.95	5.43	6.02	10.90										
	17.9	686.25	7.62	7.73	1.55										
	18.2	692.44	12.03	8.68	27.79										
	19.3	713.00	13.59	12.72	6.42										
	20.4	730.85	15.85	17.63	11.27										

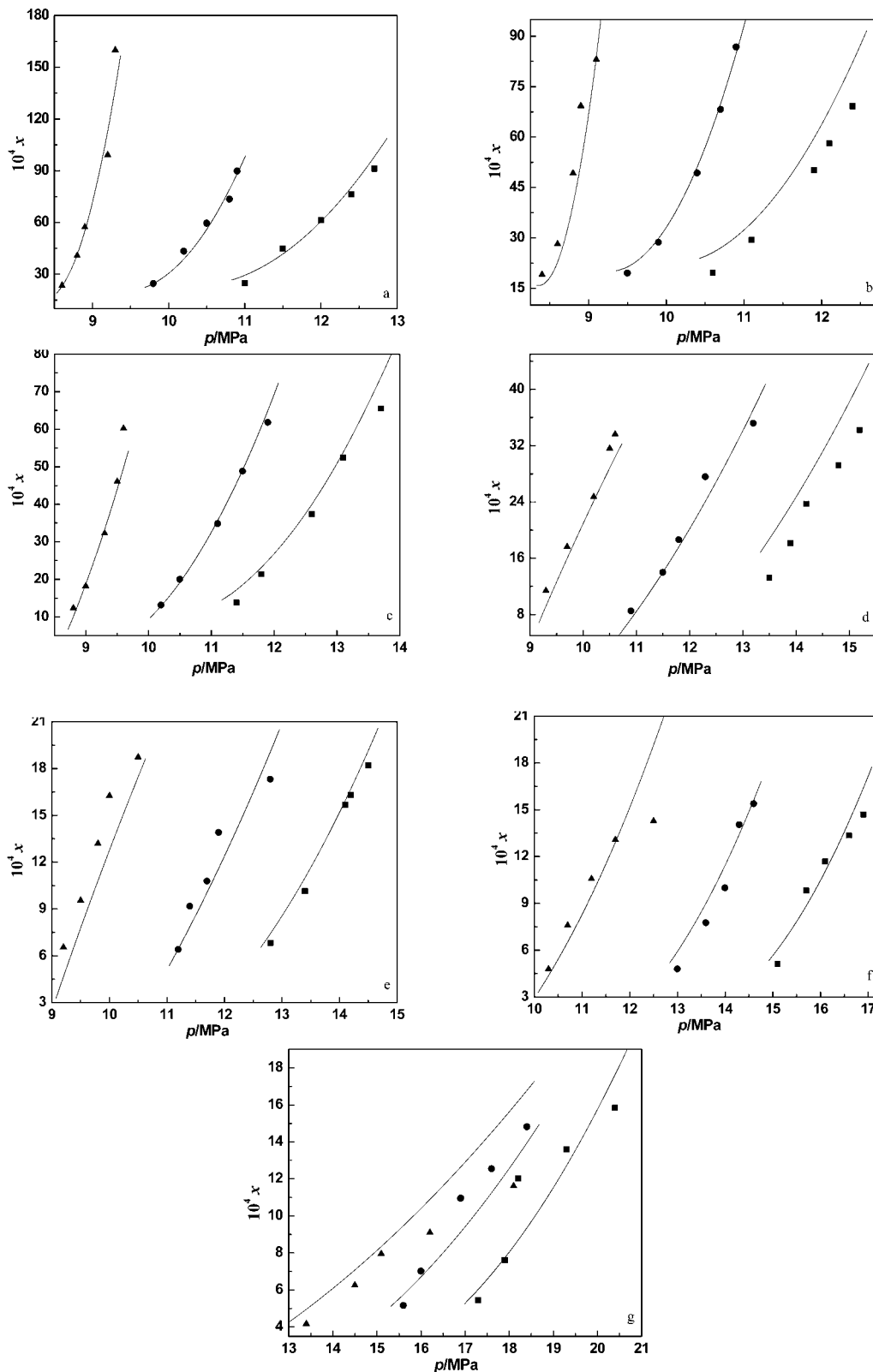


Figure 2. Comparison of solubility experimental and calculated values for compounds in supercritical CO₂ at \blacktriangle , 313 K; \bullet , 323 K; and \blacksquare , 333 K. (a) Compound 1 (dibutyl 2,2'-oxodiacetate). (b) Compound 2 (dihexyl-2,2'-oxodiacetate). (c) Compound 3 (dioctyl-2,2'-oxodiacetate). (d) Compound 4 (didecyl-2,2'-oxodiacetate). (e) Compound 5 (didodecyl-2,2'-oxodiacetate). (f) Compound 6 (ditetradecyl-2,2'-oxodiacetate). (g) Compound 7 (dihexadecyl-2,2'-oxodiacetate). \blacktriangle , \bullet , \blacksquare , exptl; —, calculated by eq 1, Bartle's model.

General Procedure for Synthesis of Diglycolic Acid Esters 1 to 7. The compounds 1 to 7 were synthesized according to the previously published procedure shown in Scheme 1.¹⁶ Even though five compounds (1 to 5) among seven glycolic acid esters

have been already known, their syntheses and structural identification data have not been documented well. Therefore, it is worthy that a detailed synthetic procedure and identification data by IR, ¹H NMR, ¹³C NMR, and elemental analysis are described. All

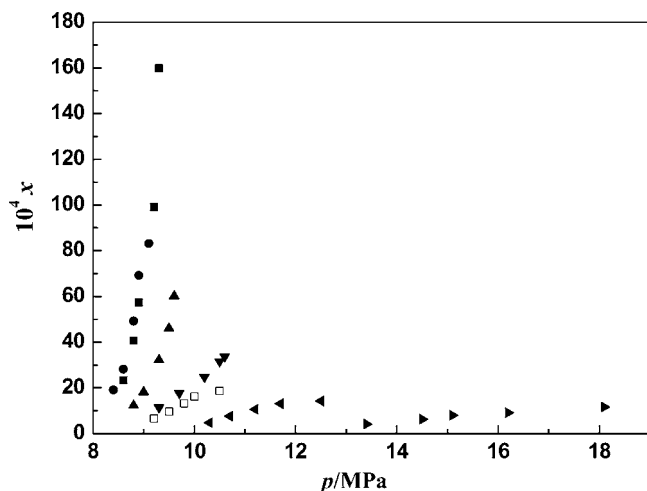


Figure 3. Solubility comparison of compounds **1** to **7** in supercritical CO_2 at 313 K. ■, Compound **1** (dibutyl 2,2'-oxidiacetate). ●, Compound **2** (dihexyl-2,2'-oxidiacetate). ▲, Compound **3** (dioctyl-2,2'-oxidiacetate). ▼, Compound **4** (didecyl-2,2'-oxidiacetate). □, Compound **5** (didodecyl-2,2'-oxidiacetate). Solid triangle pointing left, Compound **6** (ditetradecyl-2,2'-oxidiacetate). Solid triangle pointing right, Compound **7** (dihexadecyl-2,2'-oxidiacetate).

seven compounds prepared were highly pure (over $w = 0.99$ checked by GC-MS) enough to do the solubility test.

Synthesis of Dibutyl 2,2'-Oxidiacetate (1). Diglycolic acid (2.0 g, 0.015 mol) and SOCl_2 (40 mL, 0.55 mol) were stirred at circumfluence temperature for 8 h. Excess thionyl chloride was evaporated using a rotary evaporator, and then the residue was added dropwise to a CH_2Cl_2 solution (30 mL) of 1-butanol (2.7 mL, 30 mmol) and triethylamine (0.7 mL, 5 mmol) under a N_2 atmosphere. After stirring overnight, it was washed with 1 % aq. HCl, saturated aq. NaHCO_3 , and then twice with water. The collected organic phase was dried over anhydrous Na_2SO_4 and concentrated in vacuum. The residue was purified by silica gel column chromatography (ethyl acetate/petroleum ether = 1:2) to obtain a light yellow oil. Yield: $w = 0.85$, mass fraction. FT-IR (KBr, cm^{-1}): 1752.9 ($\text{C}=\text{O}$). ^1H NMR (600 MHz, CDCl_3): δ 4.24 (s, 4H, $2 \times \text{O}=\text{CCH}_2\text{O}$), 4.17 (t, 4H, $J = 6.6$, $2 \times \text{CH}_2\text{O}$), 1.61–1.66 (m, 4H, $2 \times \text{CH}_2$), 1.36–1.41 (m, 4H, $2 \times \text{CH}_2$), 0.93 (t, 6H, $J = 7.2$, $2 \times \text{CH}_3$). ^{13}C NMR (400 MHz, CDCl_3): δ_{C} 169.38, 67.34, 64.18, 29.95, 18.43, 12.96. Elemental Anal.: Calcd. for $\text{C}_{12}\text{H}_{22}\text{O}_5$ (mass fraction): C, $w = 0.5852$; H, $w = 0.90$; O, $w = 0.3248$. Found: C, $w = 0.5850$; H, $w = 0.904$; O, $w = 0.3245$.

The other compounds **2** to **7** had been prepared with the same procedure.

Dihexyl-2,2'-oxidiacetate (2). A light yellow oil with $w = 0.82$ (mass fraction) yield. FT-IR (KBr, cm^{-1}): 1751.9 ($\text{C}=\text{O}$). ^1H NMR (400 MHz, CDCl_3): δ 4.24 (s, 4H, $2 \times \text{O}=\text{CCH}_2\text{O}$), 4.16 (t, 4H, $J = 6.8$, $2 \times \text{CH}_2\text{O}$), 1.63–1.66 (m, 4H, $2 \times \text{CH}_2$), 1.30–1.36 (m, 12H, $6 \times \text{CH}_2$), 0.89 (t, 6H, $J = 6.8$, $2 \times \text{CH}_3$). ^{13}C NMR (400 MHz, CDCl_3): δ_{C} 169.37, 67.58, 64.61, 30.95, 28.08, 25.07, 22.07, 13.49. Elemental Anal.: Calcd. for $\text{C}_{16}\text{H}_{30}\text{O}_5$: C, 63.55; H, 10.00; O, 26.45 %. Found: C, 63.54; H, 10.02; O, 26.46 %.

Dioctyl-2,2'-oxidiacetate (3). A light yellow oil with $w = 0.79$ (mass fraction) yield. FT-IR (KBr, cm^{-1}): 1754.8 ($\text{C}=\text{O}$). ^1H NMR (400 MHz, CDCl_3): δ 4.24 (s, 4H, $2 \times \text{O}=\text{CCH}_2\text{O}$), 4.16 (t, 4H, $J = 6.4$, $2 \times \text{CH}_2\text{O}$), 1.61–1.66 (m, 4H, $2 \times \text{CH}_2$), 1.27–1.30 (m, 20H, $10 \times \text{CH}_2$), 0.88 (t, 6H, $J = 6.4$, $2 \times \text{CH}_3$). ^{13}C NMR (100 MHz, CDCl_3): δ_{C} 169.64, 67.89, 64.94, 31.56, 28.96, 28.34, 25.63, 22.43, 13.86. Elemental Anal.: Calcd. for

Table 2. Results of the Solubility Data Correlation Using the Bartle Model^a

compound	<i>n</i>	<i>a</i>	<i>b</i>	<i>C</i>	ΔH_{sub}	AARD
			K	$\text{m}^3 \cdot \text{kg}^{-1}$	$\text{kJ} \cdot \text{mol}^{-1}$	%
1	15	13.52	-3681.69	0.010563	30.61	6.70
2	15	14.67	-4115.98	0.009777	34.22	12.77
3	15	21.23	-6544.57	0.001033	54.41	7.60
4	15	21.21	-6872.47	0.011913	57.14	14.28
5	15	20.59	-6840.69	0.01092	56.87	11.29
6	15	24.11	-8206.5	0.020573	68.23	11.96
7	15	32.17	-11273.4	0.021407	93.72	13.32

^a Number of data points used in the correlation (*n*), parameters of the Bartle model (*a*, *b*, and *C*), average absolute relative deviations (AARD), and ΔH_{sub} (the enthalpy of sublimation of the solid solute).

$\text{C}_{20}\text{H}_{38}\text{O}_5$ (mass fraction): C, 67.00; H, 10.68; O, 22.31 %. Found: C, 67.01; H, 10.65; O, 22.33 %.

Didecyl-2,2'-oxidiacetate (4). A light yellow solid with $w = 0.81$ (mass fraction) yield. mp: 39.2 °C. FT-IR (KBr, cm^{-1}): 1755.1 ($\text{C}=\text{O}$). ^1H NMR (100 MHz, CDCl_3): δ 4.24 (s, 4H, $2 \times \text{O}=\text{CCH}_2\text{O}$), 4.16 (t, 4H, $J = 6.8$, $2 \times \text{CH}_2\text{O}$), 1.63–1.66 (m, 4H, $2 \times \text{CH}_2$), 1.26–1.30 (m, 28H, $14 \times \text{CH}_2$), 0.88 (t, 6H, $J = 6.4$, $2 \times \text{CH}_3$). ^{13}C NMR (400 MHz, CDCl_3): δ_{C} 169.74, 68.02, 65.09, 31.79, 29.40, 29.20, 29.12, 28.44, 25.73, 22.58, 14.00. Elemental Anal.: Calcd. for $\text{C}_{24}\text{H}_{46}\text{O}_5$ (mass fraction): C, 69.52; H, 11.18; O, 19.29 %. Found: C, 69.51; H, 11.19; O, 19.28 %.

Didodecyl-2,2'-oxidiacetate (5). A light yellow solid with $w = 0.82$ (mass fraction) yield. mp: 41.5 °C. FT-IR (KBr, cm^{-1}): 1751.3 ($\text{C}=\text{O}$). ^1H NMR (400 MHz, CDCl_3): δ 4.24 (s, 4H, $2 \times \text{O}=\text{CCH}_2\text{O}$), 4.16 (t, 4H, $J = 6.8$, $2 \times \text{CH}_2\text{O}$), $\delta = 1.63$ –1.66 (m, 4H, $2 \times \text{CH}_2$), 1.26–1.30 (m, 36H, $18 \times \text{CH}_2$), 0.88 (t, 6H, $J = 6.8$, $2 \times \text{CH}_3$). ^{13}C NMR (100 MHz, CDCl_3): δ_{C} 169.78, 68.07, 65.14, 31.86, 29.57, 29.51, 29.44, 29.29, 29.16, 28.49, 25.77, 22.63, 14.06. Elemental Anal.: Calcd. For $\text{C}_{28}\text{H}_{54}\text{O}_5$ (mass fraction): C, 71.44; H, 11.56; O, 16.99 %. Found: C, 71.45; H, 11.58; O, 24.98 %.

Ditetradecyl-2,2'-oxidiacetate (6). A light yellow solid with $w = 0.72$ (mass fraction) yield. mp: 46.8 °C. FT-IR (KBr, cm^{-1}): 1752.8 ($\text{C}=\text{O}$). ^1H NMR (400 MHz, CDCl_3): $\delta = 4.24$ (s, 4H, $2 \times \text{O}=\text{CCH}_2\text{O}$), xxx (t, 4H, $J = 6.8$, $2 \times \text{CH}_2\text{O}$), 1.63–1.64 (m, 4H, $2 \times \text{CH}_2$), 1.23–1.30 (m, 44H, $22 \times \text{CH}_2$), 0.88 (t, 6H, $J = 6.8$, $2 \times \text{CH}_3$). ^{13}C NMR (100 MHz, CDCl_3): δ_{C} 169.65, 67.95, 64.99, 31.81, 29.54, 29.45, 29.38, 29.25, 29.10, 28.42, 25.71, 22.56, 13.97. Elemental Anal.: Calcd. For $\text{C}_{32}\text{H}_{62}\text{O}_5$ (mass fraction): C, 72.95; H, 11.86; O, 15.18 %. Found: C, 72.94; H, 11.87; O, 15.19 %.

Dihexadecyl-2,2'-oxidiacetate (7). A light yellow solid with $w = 0.65$ (mass fraction) yield. mp: 50.1 °C. FT-IR (KBr, cm^{-1}): 1753.1 ($\text{C}=\text{O}$). ^1H NMR (400 MHz, CDCl_3): δ 4.24 (s, 4H, $2 \times \text{O}=\text{CCH}_2\text{O}$), 4.17 (t, 4H, $J = 6.8$, $2 \times \text{CH}_2\text{O}$), 1.63–1.68 (m, 4H, $2 \times \text{CH}_2$), 1.36–1.41 (m, 52H, $26 \times \text{CH}_2$), 0.88 (t, 6H, $J = 6.4$, $2 \times \text{CH}_3$). ^{13}C NMR (100 MHz, CDCl_3): δ_{C} 169.70, 68.01, 65.07, 31.85, 29.62, 29.49, 29.42, 29.29, 29.14, 28.46, 25.75, 22.61, 14.02. Elemental Anal.: Calcd. for $\text{C}_{36}\text{H}_{70}\text{O}_5$ (mass fraction): C, 74.17; H, 12.10; O, 13.72 %. Found: C, 74.15; H, 12.12; O, 13.74 %.

Procedure for Solubility Test in Supercritical CO_2 . The solubilities of all the seven compounds were tested using the static analytical method. For observation of dissolution of the compounds in scCO_2 , a high-pressure view cell consisting of a stainless steel block with two sapphire windows was used (Figure 1). A suitable amount of compound and a magnetic stirring bar were placed into the cell (7.11 mL). The cell was then purged with CO_2 to remove the air and sealed. The system was heated to the desired temperature using a temperature

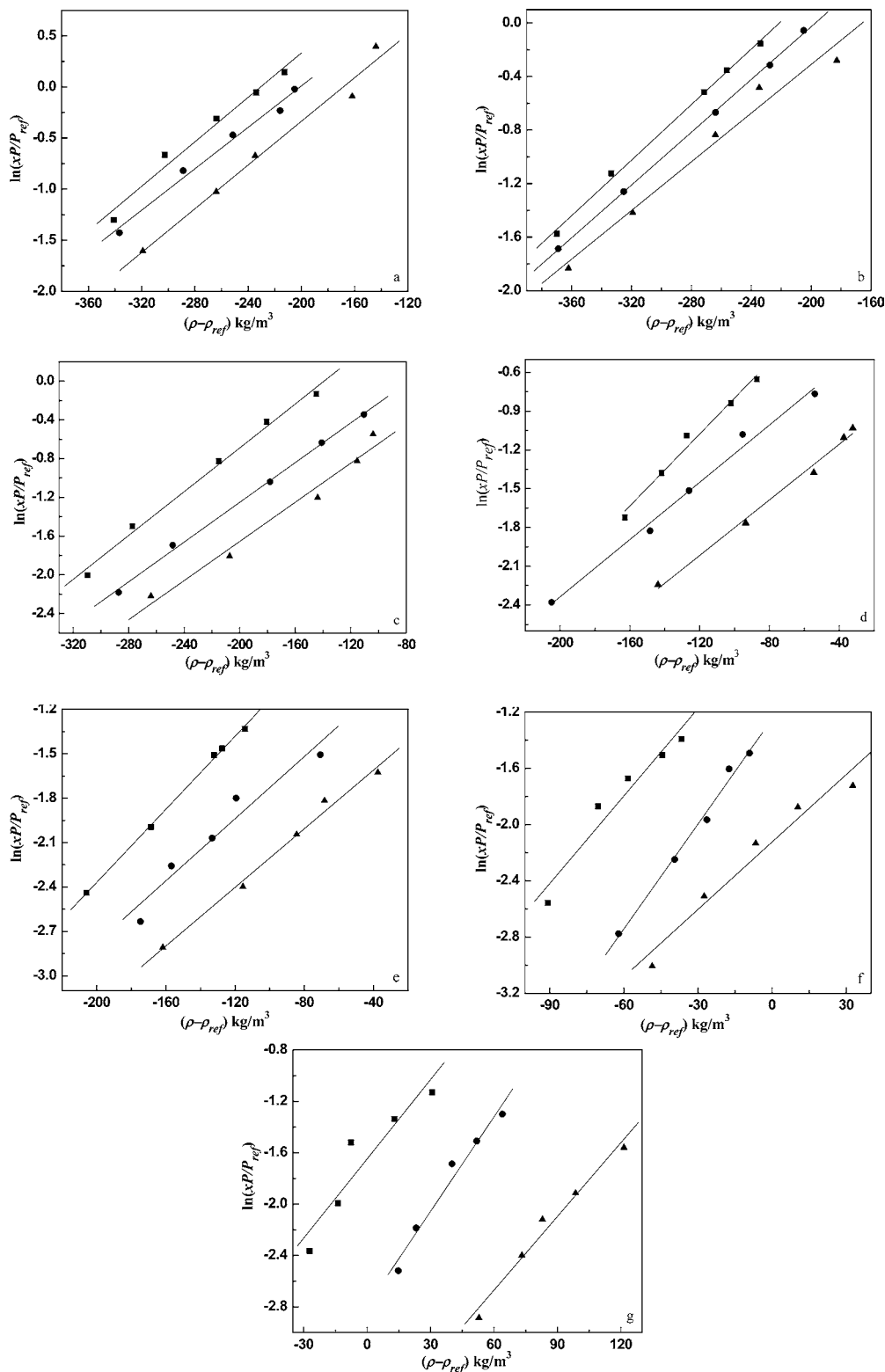


Figure 4. Plots of $\ln(xP/P_{\text{ref}})$ vs $(\rho - \rho_{\text{ref}})/\text{kg}\cdot\text{m}^{-3}$ via eq 1 for compounds 1 to 7 at various temperatures. x , mole fraction of compounds; P , CO_2 pressure; P_{ref} , 0.1 MPa; ρ , density of pure CO_2 ; ρ_{ref} , $700 \text{ kg}\cdot\text{m}^{-3}$. (a) Compound 1, (b) Compound 2, (c) Compound 3, (d) Compound 4, (e) Compound 5, (f) Compound 6, (g) Compound 7. \blacktriangle , 313 K; \bullet , 323 K; \blacksquare , 333 K, Bartle model.

circulating bath jacket, and the solution was allowed to equilibrate while being stirred. The pressure was increased gradually until the system became a homogeneous transparent single phase. When the pressure kept constant for a period of time, 20 min, the pressure was recorded and defined as the dissolution pressure. At each condition, the experiment was repeated at least three times. The dissolution pressure and

temperature were recorded to obtain the density of CO_2 from the Web site.¹⁷ The uncertainty of the dissolution pressure and temperature was ± 0.5 MPa and ± 0.1 °C, respectively.

Results and Discussion

Solubility Results. The solubility of the compounds in scCO_2 was tested at (313, 323, and 333) K and the pressure range from

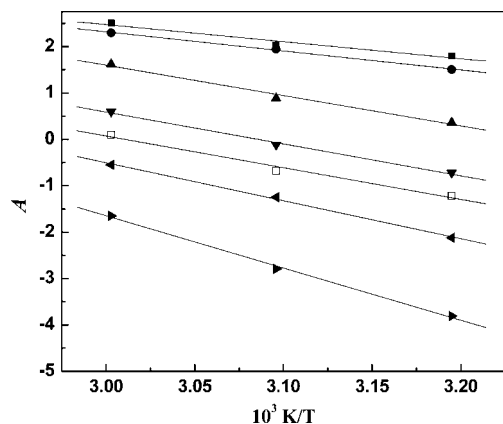


Figure 5. Plots of A vs $1000/T$ for compounds. ■, Compound 1 (dibutyl 2,2'-oxidiacetate). ●, Compound 2 (dihexyl-2,2'-oxidiacetate). ▲, Compound 3 (dioctyl-2,2'-oxidiacetate). ▼, Compound 4 (didecyl-2,2'-oxidiacetate). □, Compound 5 (didodecyl-2,2'-oxidiacetate). Solid triangle pointing left, Compound 6 (ditetradecyl-2,2'-oxidiacetate). Solid triangle pointing right, Compound 7 (dihexadecyl-2,2'-oxidiacetate).

(8.6 to 20.4) MPa. The experimental results are shown in Figure 2 and Table 1, and the mole fractions of the compounds were reproducible within $\pm 3\%$. The results showed that the solubilities of compounds increased with the increase of pressure at constant temperature. For example, the mole fraction solubility of dibutyl 2,2'-oxidiacetate (compound 1) at 313 K drastically increased from $2.3 \cdot 10^{-3} \text{ mol} \cdot \text{L}^{-1}$ at 8.6 MPa to $1.6 \cdot 10^{-2} \text{ mol} \cdot \text{L}^{-1}$ at 9.3 MPa because of a rapid increase in density with pressure. In contrast, at the same pressure the solubilities of compounds decreased with the increase of temperature as shown in Figure 2.

In line with our expectation, the solubility sequence was observed as $1 > 2 > 3 > 4 > 5 > 6 > 7$ (Figure 3). For example, at 313 K, the solubility of dibutyl 2,2'-oxidiacetate (1) reached $1.6 \cdot 10^{-2} \text{ mol} \cdot \text{L}^{-1}$ at 9.3 MPa, dihexyl-2,2'-oxidiacetate (2) $8.3 \cdot 10^{-3} \text{ mol} \cdot \text{L}^{-1}$ at 9.1 MPa, dioctyl-2,2'-oxidiacetate (3) $1.8 \cdot 10^{-3} \text{ mol} \cdot \text{L}^{-1}$ at 9.0 MPa, didecyl-2,2'-oxidiacetate (4) $1.1 \cdot 10^{-3} \text{ mol} \cdot \text{L}^{-1}$ at 9.3 MPa, didodecyl-2,2'-oxidiacetate (5) $6.5 \cdot 10^{-4} \text{ mol} \cdot \text{L}^{-1}$ at 9.0 MPa, ditetradecyl-2,2'-oxidiacetate (6) $4.7 \cdot 10^{-4} \text{ mol} \cdot \text{L}^{-1}$ at 10.3 MPa, and dihexadecyl-2,2'-oxidiacetate (7) $4.1 \cdot 10^{-3} \text{ mol} \cdot \text{L}^{-1}$ at 13.4 MPa. It was obvious that the solubility of the compounds decreased with the increase of the length of hydrocarbon chain at the same temperature and pressure. This phenomenon was consistent with Shen's¹⁸ and Chang's¹⁹ description.

Correlation of Experimental Solubility Data. Density-Based Correlations of Solubility Data. To correlate the solubility data, two density-based correlations proposed by Bartle and Chrastil were investigated for the seven glycolic acid esters. The literature has already provided many examples in which these models were investigated.^{20–23}

Bartle et al. Model. Bartle and co-workers²³ proposed a simple density-based semiempirical model to correlate the solubility of solids in SCFs:

The experimental solubility data for the seven compounds were correlated using the following equation

$$\ln(xP/P_{\text{ref}}) = A + C(\rho - \rho_{\text{ref}}) \quad (1)$$

where

$$A = a + b/T \quad (2)$$

where x was the mole fraction of the solutes; P was the pressure; P_{ref} was 0.1 MPa; ρ was the density of pure CO_2 at the experimental temperature and pressure; ρ_{ref} was $700 \text{ kg} \cdot \text{m}^{-3}$; and A , C , a , and b were constants. In the initial stage, $\ln(xP/P_{\text{ref}})$ values were plotted against $(\rho - \rho_{\text{ref}})$ (Figure 4), and the values were fitted with a straight line by least-squares regression to estimate the C and A parameters. The values of C , obtained from the slopes of the corresponding plots, were then averaged for each compound (Table 2). When C was held at its average value, the experimental solubility data were then used to evaluate the A values at various temperatures for each compound. The plots of A versus $1/T$ for each compound were fitted to a straight line (Figure 5) from which the intercept and the slope (a and b) were obtained. The resulting a and b values for compounds were also shown in Table 2. The values of a , b , and C were used to predict solubility using eq 1 and eq 2. In this model, the parameter b is related to the enthalpy of sublimation of the solute, ΔH_{sub} , by the expression $\Delta H_{\text{sub}} = -Rb$, where R is the gas constant.

The calculated data and the experimental data were compared in Figure 2. Finally, the average absolute relative deviation (AARD) was used to test the correlation results. It was calculated with the following eq 3

$$\text{AARD} = 1/n \sum |x_{i,\text{cal}} - x_{i,\text{exp}}|/x_{i,\text{exp}} \cdot 100\% \quad (3)$$

where n was the number of experimental points and $x_{i,\text{cal}}$ and $x_{i,\text{exp}}$ were the calculated and experimental data, respectively. The values of AARD were in the range of (3 to 25) %.

Chrastil Model. The model proposed by Chrastil relates the solubility of the solute to the density of the supercritical solvent on the assumption that one molecule of a solute, A , associates with k molecules of solvent, B , to form a solvate complex AB_k , in equilibrium with the system.^{24–27}

In this model, the experimental solubility data for the seven compounds were correlated using the following eq 4

Table 3. Results of the Solubility Data Correlation Using the Chrastil Model^a

compound	n	k	α		β	σ^2	ΔH	AARD
			K				$\text{kJ} \cdot \text{mol}^{-1}$	%
1	15	5.36288	-1602.552		-25.1009	0.98029	13.32361	6.62546
2	15	4.65949	-581.3433		-23.7861	0.99443	4.83328	3.26356
3	15	5.60836	-3682.655		-20.8929	0.98733	30.61759	5.31947
4	15	6.71614	-2621.435		-32.2818	0.97539	21.79461	5.56868
5	15	6.53948	-3039.141		-30.1439	0.9732	25.26742	5.38784
6	15	12.28923	-5071.91		-62.1419	0.90526	42.16786	10.84257
7	15	13.94997	-9558.331		-60.3894	0.89329	79.46796	10.39084

^a Number of data points used in the correlation (n), parameters of the Chrastil model (k , α , and β), average absolute relative deviations (AARD), regression coefficients σ^2 , and ΔH (sum of the heat of vaporization and heat of solvation of the solute).

$$\ln S = k \ln \rho + (\alpha/T) + \beta \quad (4)$$

where the solubility, S , is calculated by means of eq 5

$$S = (\rho M_2 x)/(M_1(1 - x)) \quad (5)$$

where x is the molar fraction of the solute and M_1 and M_2 are the molecular weights of CO_2 and the solute, respectively. The

constants α , β , and k can be estimated from the experimental solubility data in scCO_2 . In eqs 4 and 5, ρ ($\text{kg}\cdot\text{m}^{-3}$) is the density of the pure scCO_2 ; S ($\text{kg}\cdot\text{m}^{-3}$) is the solubility of the solid in the supercritical phase; T is the temperature in K; and k , α , and β are the adjustable parameters of the model. The constant k is the association number, α a constant, defined as $-\Delta H/R$ (where ΔH is the sum of the enthalpies of vaporization and solvation of the solute and R the gas constant), and β

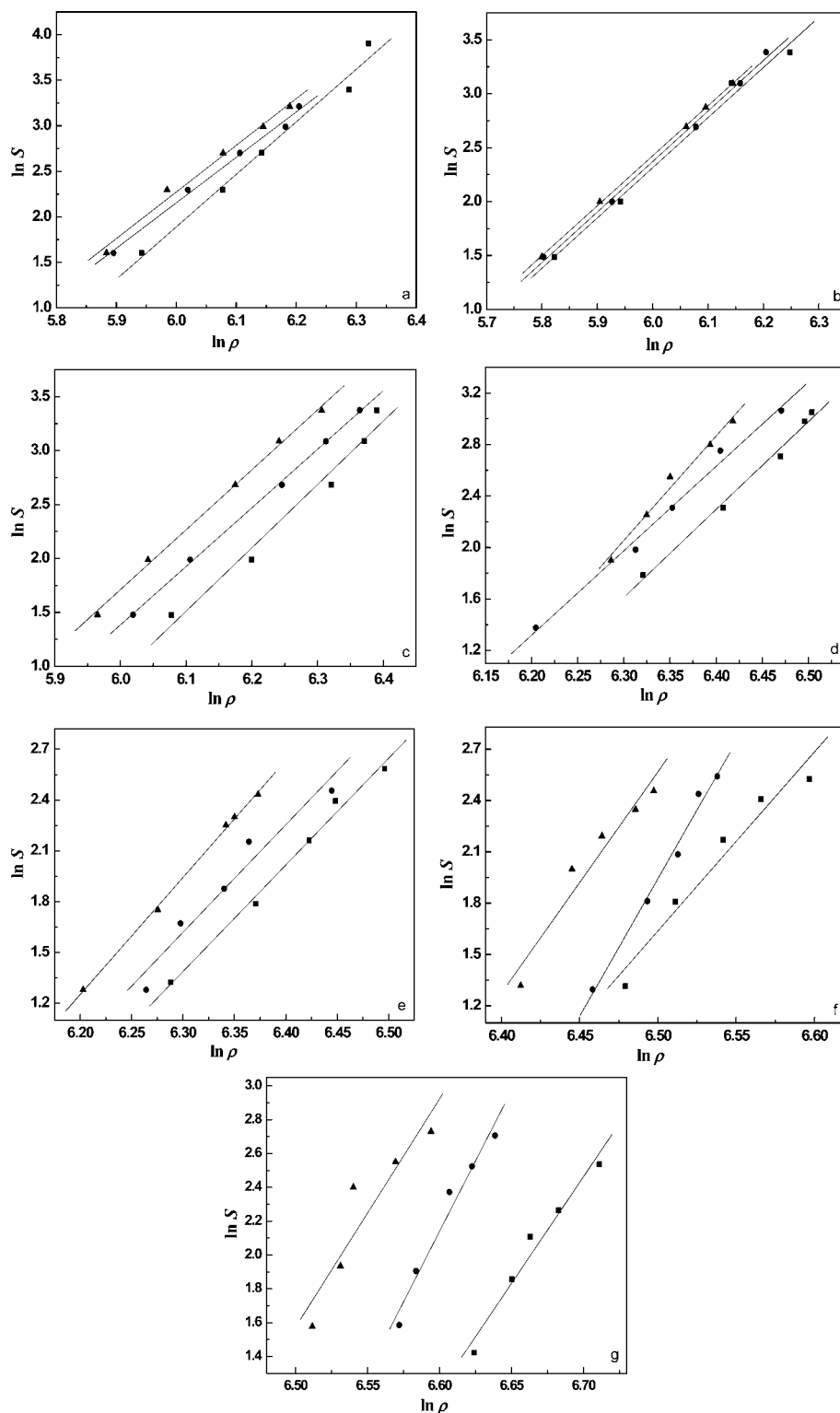


Figure 6. Plots of $\ln S$ vs $\ln \rho$ via eq 4 for the seven compounds at \blacksquare , 313 K; \bullet , 323 K; \blacktriangle , 333 K, Chrastil model. (a) Compound 1 (dibutyl 2,2'-oxidiacetate). (b) Compound 2 (dihexyl-2,2'-oxidiacetate). (c) Compound 3 (dioctyl-2,2'-oxidiacetate). (d) Compound 4 (didecyl-2,2'-oxidiacetate). (e) Compound 5 (didodecyl-2,2'-oxidiacetate). (f) Compound 6 (ditetradecyl-2,2'-oxidiacetate). (g) Compound 7 (dihexadecyl-2,2'-oxidiacetate).

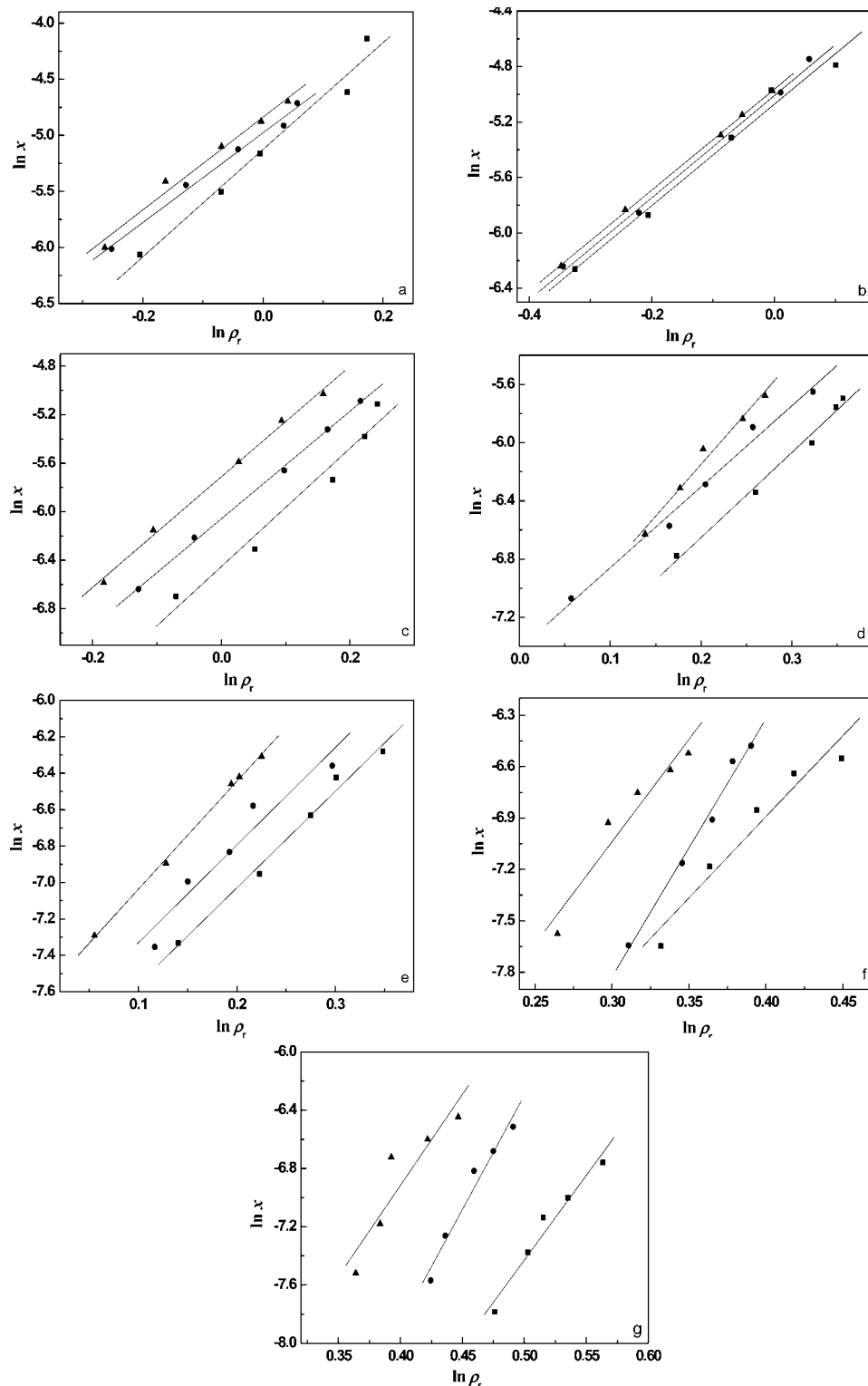


Figure 7. Plots of $\ln x$ vs $\ln \rho_r$ via eq 7 for the seven compounds at \blacksquare , 313 K; \bullet , 323 K; and \blacktriangle , 333 K. (a) Compound 1 (dibutyl 2,2'-oxidiacetate). (b) Compound 2 (dihexyl-2,2'-oxidiacetate). (c) Compound 3 (dioctyl-2,2'-oxidiacetate). (d) Compound 4 (didecyl-2,2'-oxidiacetate). (e) Compound 5 (didodecyl-2,2'-oxidiacetate). (f) Compound 6 (ditetradecyl-2,2'-oxidiacetate). (g) Compound 7 (dihexadecyl-2,2'-oxidiacetate).

depends on the molecular weights of the solute and solvent. The Chrastil model suggests that plots of $\ln S$ for several temperatures are straight lines whose slopes are identical and equal to k . The parameters, k , α , and β , are obtained performing a multiple linear regression on the experimental solubility data.

The values of calculated constants for the seven diglycolic acid ester + $scCO_2$ systems are presented in Table 3. The quality of the correlation is expressed in terms of σ^2 and the average absolute

relative deviations (AARD) between experimental and calculated solubility S . The consistency of the model with measured data can be seen from Figure 6 and the values of AARD at different temperatures, which are less than 11 %. The results exhibited a good agreement between the tested and calculated data.

Estimation of the Partial Molar Volumes of the Solutes. The partial molar volumes of the solutes are very important parameters for the solubility evaluation of solutes in SCF.

Although our compounds reported here are new and the corresponding data of partial molar volumes are nonavailable from the literature, it is still useful and interesting for other scientists to refer to in the future. So, the partial molar volumes of the seven new compounds were calculated as follows.

According to Kumar and Johnston,²⁸ the dependence of the solubility x of the solute with its partial molar volume in the vicinity of the critical density of the SCF can be expressed by the following equation

$$\ln x = -C_2 + \ln\left(\frac{P_2^{VP}}{\rho_c RT}\right) + \frac{PV_2^s}{RT} - \left(\frac{\bar{V}_2}{RT\kappa_T}\right)_{\rho_r=1} \ln \rho_r \quad (6)$$

where x represents the equilibrium mole fraction of the solute in the SCF; P_2^s and V_2^s are the vapor pressure and molar volume of the solid solute; R is the universal gas constant; \bar{V}_2 is the partial molar volume of the solute in the SCF phase; $\kappa_T = [(1/\rho)(\partial\rho/\partial P)_{T,x}]$ and $\rho_r = \rho/\rho_c$ are the isothermal compressibility and reduced density of the phase; and T is the operating temperature.

The partial molar volumes of the solute in the SCF phase, \bar{V}_2 , are much larger than the molar volume of the solute, V_2^s . The third term in eq 6 was considered as constant in the region of interest. Equation 6 may thus be simplified as

$$\ln x = C_0 - \left(\frac{\bar{V}_2}{RT\kappa_T}\right)_{\rho_r=1} \ln \rho_r \quad (7)$$

Equation 7 implies that in the approximate density interval $0.5 \leq \rho_r \leq 2.0$ the log of the mole fraction of the solubility of the solute in an SCF varies linearly with the log of the density of the SCF phase. The slope of this line is the ratio of the partial molar volume of the solute in the SCF phase to the isothermal compressibility of the fluid phase. This ratio is considered as independent of ρ_r , thus the knowledge of the value of κ_T and the slope of the $\ln x$ versus $\ln \rho_r$ at this temperature permits the estimation of \bar{V}_2 under these conditions. As demonstrated in Figure 7, the systems investigated display linearity when plotted as $\ln x$ versus $\ln \rho_r$. This linearity is not observed when $\ln x$ values were plotted versus ρ_r . The slopes of the line $\ln x$ versus $\ln \rho_r$ were computed by linear squares fit for the seven diglycolic acid esters + scCO₂ systems at different temperatures. The quality of the linear correlation is expressed in terms of σ^2 . Partial molar volumes were then deduced from the determined slopes and the values of κ_T for CO₂ at the appropriate P – T conditions.

The results obtained are recapitulated in Table 4. As shown in Table 4, the partial molar volume for each solute decreases as temperature increases. The partial molar volumes \bar{V}_2 of the seven diglycolic acid esters in the vicinity of the critical point of the solvent, which are difficult to measure experimentally, are then estimated by following the theory developed by Kumar and Johnston. As reported by these authors,²⁷ the data calculated for naphthalene + CO₂ and naphthalene + ethylene systems according to this theory were in good agreement with experimental data. However, the calculation results of this work necessitate a confrontation with experimental measurements by other scientists.

Conclusion

In the present study, we have designed and synthesized seven new CO₂-philic diglycolic acid esters containing nonfluorous

Table 4. Slopes Computed from Equation 7 and the Corresponding Partial Molar Volumes \bar{V}_2 of the Solute for Each Diglycolic Acid Ester + scCO₂ System at Different Temperatures

compound	T	slope at $\rho_r = 1$	σ^2	\bar{V}_2
1	313	4.76789	0.96683	-7116.36
	323	3.99274	0.98699	-2588.95
	333	4.12654	0.97746	-1697.88
2	313	3.65393	0.97912	-5453.71
	323	3.68054	0.99328	-2386.52
	333	3.63807	0.99931	-1496.89
3	313	4.87481	0.95083	-7275.95
	323	4.43524	0.99797	-2875.88
	333	4.55835	0.99505	-1875.55
4	313	5.83963	0.98475	-8716
	323	5.56119	0.98293	-3605.96
	333	7.11716	0.97566	-2928.37
5	313	5.2974	0.98333	-7906.69
	323	5.35681	0.90786	-3473.44
	333	5.92027	0.9974	-2435.91
6	313	9.47104	0.92379	-14136.1
	323	15.06431	0.98296	-9767.93
	333	11.94743	0.9088	-4915.8
7	313	11.62306	0.94638	-17348.1
	323	15.6659	0.94918	-10158
	333	12.49359	0.79132	-5140.52

alkyl groups. The solubilities of these compounds were measured at the temperature from (313 to 333) K and in the pressure range of (8.6 to 20.4) MPa. All of these derivatives showed high solubilities in supercritical CO₂ at easily accessible temperatures and pressures. The measured data were correlated with two density-based models (Bartle and Chrastil models) which were able to successfully correlate the experimental solubility data, and the results showed good agreement between the correlated results and the experimental data. Better agreement with experimental solubility data is obtained with Chrastil model, and values of AARD lower than 11 % were observed. Solubility data were also used to estimate the partial molar volume \bar{V}_2 for each diglycolic acid ester in the supercritical phase using the theory developed by Kumar and Johnston. This work might provide basic information for designing and synthesizing new low-cost, nonfluorous, CO₂-philic compounds.

Acknowledgment

H. Kim thanks Kyung Hee University (Korea) for a sabbatical year (2009).

Literature Cited

- (1) Porto, C. D.; Decorti, D.; Kikic, I. Flavour Compounds of Lavandula Angustifolia L. to Use in Food Manufacturing: Comparison of Three Different Extraction Methods. *Food Chem.* **2009**, *112*, 1072–1078.
- (2) Wang, W.; Yang, H.-J.; Hu, J.; Guo, C.-Y. Solubilities of Diglycolic Acid Esters at Temperatures Ranging From (343 to 363) K in Supercritical Carbon Dioxide. *J. Chem. Eng. Data* **2010**, *55*, 694–697.
- (3) Sarbu, T.; Styraneac, T.; Beckman, E. J. Non-fluorous Polymers with Very High Solubility in Supercritical CO₂ Down to Low Pressures. *Nature* **2000**, *405*, 165–168.
- (4) Beckman, E. J. Supercritical and Near-critical CO₂ in Green Chemical Synthesis and Processing. *J. Supercrit. Fluids* **2004**, *28*, 121–191.
- (5) Du, Y.; Cai, F.; Kong, D. L.; He, L. N. Organic Solvent-free Process for the Synthesis of Propylene Carbonate from Supercritical Carbon Dioxide and Propylene Oxide Catalyzed by Insoluble Ion Exchange Resins. *Green Chem.* **2005**, *7*, 518–523.
- (6) Erkey, C. Supercritical Carbon Dioxide Extraction of Metals from Aqueous Solutions: a Review. *J. Supercrit. Fluids.* **2000**, *17*, 259–287.
- (7) Yang, H.-J.; Kim, H.; Guo, C.-Y. Metal Ion Extraction with Bipyridine Derivatives as Chelating Ligands in Supercritical Carbon Dioxide. *Clean* **2010**, *38*, 159–166.
- (8) Wang, W.; Yang, H.-J.; Hu, J.; Guo, C.-Y. Extraction of Metal Ions with Non-fluorous Bipyridine Derivatives as Chelating Ligands in Supercritical Carbon Dioxide. *J. Supercrit. Fluids* **2009**, *51*, 181–187.

- (9) Beckman, E. J. A Challenge for Green Chemistry: Designing Molecules that Readily Dissolve in Carbon Dioxide. *Chem. Commun.* **2004**, 1885–1888.
- (10) Raveendran, P.; Wallen, S. Sugar Acetates as Novel, Renewable CO₂-Philes. *J. Am. Chem. Soc.* **2002**, *124*, 7274–7275.
- (11) Eastoe, J.; Dupont, A.; Steyler, D. C. Fluorinated Surfactants in Supercritical CO₂. *Curr. Opin. Colloid Interface Sci.* **2003**, *8*, 267–273.
- (12) Zhang, Y.; Cangul, B.; Garrabos, Y.; Erkey, C. Thermodynamics and kinetics of adsorption of bis(2,2,6,6-tetramethyl-3,5-heptanedionato) (1,5-cyclooctadiene) ruthenium (II) on carbon aerogel from supercritical CO₂ solution. *J. Supercrit. Fluids* **2008**, *44*, 71–77.
- (13) Liu, J.; Han, B.; W, Z.; Zhang, J.; Li, G.; Yang, G. Solubility of Ls-45 Surfactants in Supercritical CO₂ and Loading Water in the CO₂/Water/Surfactant Systems. *Langmuir* **2002**, *18*, 3086–3089.
- (14) Xie, Y.; Yang, H. J.; Wang, W.; Chen, R. Solubilities of Diglycolic Acid Esters in Supercritical Carbon Dioxide. *J. Chem. Eng. Data* **2009**, *54*, 102–107.
- (15) Smart, N. G.; Carleson, T. E.; Elshani, S.; Wang, S.; Wai, C. M. Extraction of Toxic Heavy Metals Using Supercritical Fluid Carbon Dioxide Containing Organophosphorus Reagents. *Ind. Eng. Chem. Res.* **1997**, *36*, 1819–1826.
- (16) Liu, J. F.; Yang, H. J.; Wang, W.; Li, Z. Solubilities of Amide Compounds in Supercritical Carbon Dioxide. *J. Chem. Eng. Data* **2008**, *53*, 2189–2192.
- (17) <http://www.nist.gov/srd/fluids.htm> (accessed June 25, 2009).
- (18) Shen, Z. H.; McHugh, M. A.; Lott, K. M.; Wright, M. E. Solubility of Semi-fluorinated and Nonfluorinated Alkyl Dichlorobenzoates in Supercritical CO₂. *Fluid Phase Equilib.* **2004**, *216*, 1–12.
- (19) Chang, F.; Kim, H.; Joo, B.; Park, K.; Kim, H. Novel CO₂-soluble Pyridine Derivatives and the Extraction of Heavy Metals into SC-CO₂. *J. Supercrit. Fluids* **2008**, *45*, 43–50.
- (20) Miller, D. J.; Hawthorne, S. B.; Clifford, A. A.; Zhu, S. Solubility of Polycyclic Aromatic Hydrocarbons in Supercritical Carbon Dioxide from 313 to 523 K and from 100 to 450 bar. *J. Chem. Eng. Data* **1996**, *41*, 779–786.
- (21) Huang, Z.; Yang, X.-W.; Sun, G.-B.; Song, S.-W.; Kawi, S. The Solubilities of Xanthone and Xanthene in Supercritical Carbon Dioxide. Structure Effect. *J. Supercrit. Fluids* **2005**, *36*, 91–97.
- (22) Bai, Y.; Yang, H. J.; Quan, C.; Guo, C. Y. Solubilities of 2,2'-Bipyridine and 4,4'-Dimethyl-2,2'-bipyridine in Supercritical Carbon Dioxide. *J. Chem. Eng. Data* **2007**, *52*, 2074–2076.
- (23) Bartle, K. D.; Clifford, A. A.; Jafar, S. A.; Shilstone, G. F. Solubilities of Solids and Liquids of Low Volatility in Supercritical Carbon Dioxide. *J. Chem. Phys. Data* **1991**, *20*, 713–756.
- (24) Coimbra, P.; Fernandes, D.; Ferreira, P.; Gil, M. H.; Sousa, H. C. Solubility of Irgacure® 2959 Photoinitiator in Supercritical Carbon Dioxide: Experimental Determination and Correlation. *J. Supercrit. Fluids* **2008**, *45*, 272–281.
- (25) Li, W.; Jin, J.; Tian, G.; Zhang, Z. Single-component and Mixture Solubilities of Ethyl *p*-Hydroxybenzoate and Ethyl *p*-Aminobenzoate in Supercritical CO₂. *Fluid Phase Equilib.* **2008**, *264*, 93–98.
- (26) Khimeche, K.; Alessi, P.; Kikic, I.; Dahmani, A. Solubility of Diamines in Supercritical Carbon Dioxide: Experimental Determination and Correlation. *J. Supercrit. Fluids* **2007**, *41*, 10–19.
- (27) Chrastil, J. Solubility of Solids and Liquids in Supercritical Gases. *J. Phys. Chem.* **1982**, *86*, 3016–3021.
- (28) Kumar, S. K.; Johnston, K. P. Modeling the Solubility of Solids in Supercritical Fluids with Density as the Independent Variable. *J. Supercrit. Fluids* **1988**, *1*, 15–22.

Received for review October 26, 2009. Accepted June 29, 2010. We are grateful to the National Natural Science Foundation of China (No. 20607031). Hai-Jian Yang also wants to acknowledge the financial support from the Institute of Fine Chemicals of South-Central University for Nationalities (XJY10003).

JE900893E